

Study on the Corrosion Resistance of the H65 Copper Alloy Surface Modified by Friction Stir Surface Processing

Xiaole Ge*, Weiwei Song, Di Jiang, Shouzhen Cao, Hongfeng Wang, Shengrong Liu

College of Mechanical and Electrical Engineering, Huangshan University, Huangshan, Anhui, 245041, China

*E-mail: xiaole_ge@163.com

Received: 31 August 2021 / Accepted: 16 March 2022 / Published: 7 May 2022

The surface modification of H65 copper alloy was realized by using friction stir surface processing (FSSP) technology and a needleless tool. Electrochemical experiments and salt spray corrosion experiments were conducted to explore the influence of FSSP process parameters on the corrosion resistance of the processed surface. The electrochemical polarization curves and the salt spray corrosion depths under different FSSP process parameters were analyzed. Electron backscattered diffraction (EBSD) experiments were performed under typical process parameters to investigate the grain size distributions, dynamic recrystallization percentage and dislocation densities. The results show that the corrosion resistance of the modified surface is improved to various degrees after FSSP compared with the base metal, and the corrosion resistance is the best when the traverse speed is 100 mm/min and the rotational speed is 600 rpm. The main reasons for this are that dynamic recrystallization occurs adequately due to the high heat input, and the grain size and dislocation density are significantly reduced.

Keywords: Corrosion resistance; H65 copper alloy; Friction stir surface processing; Process parameters

1. INTRODUCTION

Copper alloys are widely used in many fields, such as the shipbuilding industry, the energy and chemical industry, and the rail transit industry, due to their good mechanical properties, high ductility and excellent electrical and thermal conductivity [1-10]. Corrosion damage is one of the most common failure forms of copper alloy parts, especially for some parts working in a corrosive environment for a long time that are more prone to damage due to surface corrosion, resulting in a reduction in their service life. Therefore, it is of great significance to carry out research on the corrosion resistance of copper alloys to slow down surface corrosion and prolong the service life of copper alloy parts.

Many researchers have investigated the corrosion resistance of copper and copper alloys. Singh

et al. prepared a graphene oxide-polymer composite coating on copper using an electrophoretic deposition method. The results indicated that the corrosion resistance of copper was effectively improved [11]. Chukwuike et al. investigated the corrosion resistance of copper surfaces by using the laser shock peening method, and the electrochemical test results demonstrated that the corrosion resistance was greatly improved compared to that of the base metal [12]. To improve the corrosion resistance of the copper surface, Hu et al. prepared an Al-Fe coating on the copper surface by using the pack cementation method and obtained a good anti-corrosion effect [13]. Xu et al. prepared a Cu/liquid microcapsule composite coating by using the electroplating method which gained superior corrosion resistance performance [14]. The above studies mainly improved the corrosion resistance of the copper surface by preparing coatings, but this method is not suitable for the surface treatment of large parts owing to the high cost and complicated production process. In view of this deficiency, friction stir processing (FSP) technology has been used by some scholars to modify the surface of metal materials to improve their corrosion resistance [15-21]. FSP, which is a variant of friction stir welding (FSW), can change the surface properties of the material by generating local plastic deformation and heat [22]. On the basis of FSP, Song et al. proposed a friction stir surface processing (FSSP) method that has been successfully applied in the surface modification of H62 copper alloy and obtained ideal surface corrosion resistance [23-24]. In previous studies, regardless of whether the metal surface was modified by FSP or FSSP, the tool only processed a section of the area along a straight line without processing a large surface. However, in practical engineering applications, especially for the surface modification of some large parts, a large modification area is necessary.

In this work, a large-area surface modification of H65 copper alloy was performed by using FSSP technology and a needleless tool. The effect of FSSP process parameters on the corrosion resistance of the processed surface was investigated. Furthermore, the microstructure changes of the modified surface under typical process parameters were analyzed. The research content can provide a reference for the practical engineering application of copper alloy surface modification.

2. EXPERIMENT

2.1 Experimental materials

An H65 copper alloy plate with dimensions of 200×100×10 mm was adopted to perform FSSP experiments. The chemical composition of the H65 copper alloy is listed in Table 1.

Table 1. Chemical composition of the H65 copper alloy (mass fraction, %)

Elements	Cu	Pb	P	Fe	Sb	Bi	Zn	Impurities
Content	63.5-68	0.03	0.01	0.1	0.005	0.005	Balance	0.3

2.2 Experimental equipment and methods

The experiments were carried out in an FSW-LM-A10-type friction stir processing machine

produced by Beijing Saifusite Co., Ltd. (China). A homemade needleless tool was utilized to process the surface of the H65 copper alloy in this paper, as shown in Figure 1.



Figure 1. Needleless tool used in experiments

To explore the influence of FSSP process parameters on the surface corrosion resistance of the H65 copper alloy, 9 experiments with different traverse speeds and rotational speeds were designed, as listed in Table 2. The tilt angle of the needleless tool and the processing depth were set to 0° and 0.5 mm, respectively.

Table 2. Process parameter settings used in experiments

Traverse speed (TS) (mm/min)	Rotational speed (RS) (rpm)	Sample number
100	200	Sample 1
100	400	Sample 2
100	600	Sample 3
200	200	Sample 4
200	400	Sample 5
200	600	Sample 6
300	200	Sample 7
300	400	Sample 8
300	600	Sample 9

The processing path of the needleless tool on the H65 copper alloy surface was A-B-C-D-E-F-G-H-I-J-K-L-M-N-O-C-P, as shown in Figure 2. The H65 copper alloy surface to be processed was cleaned before FSSP to remove the oil stains. The processed H65 copper alloy plates were cut by a DK7732PZ-type wire cutting machine produced by Suzhou Hanqi CNC Equipment Co., Ltd. to obtain the required test samples. The electrochemical corrosion test samples, salt spray corrosion test samples and electron backscattered diffraction (EBSD) test samples were extracted from different positions of the FSSP zone, and they were used to conduct the electrochemical corrosion experiments, salt spray corrosion experiments and EBSD experiments, respectively, as depicted in Figure 2.

3. RESULTS AND DISCUSSION

3.1 Analysis of the modified surface macromorphology

Figure 3 shows the macromorphologies of the H65 copper alloy under different FSSP process parameters. Figure 3 shows that the modified surfaces are all well formed under different FSSP process parameters, which lays a foundation for discussing the corrosion resistance of the modified surfaces and provides a possibility for popularizing large surface modifications. Figure 3 also shows that the knife grains on the modified surfaces are slightly different under different FSSP process parameters; the faster the traverse speed is, the larger the knife grains and the rougher the modified surface. Since the modified surfaces need to be finished to obtain the required surface quality in actual applications, the size of the knife grain will not affect the actual use.

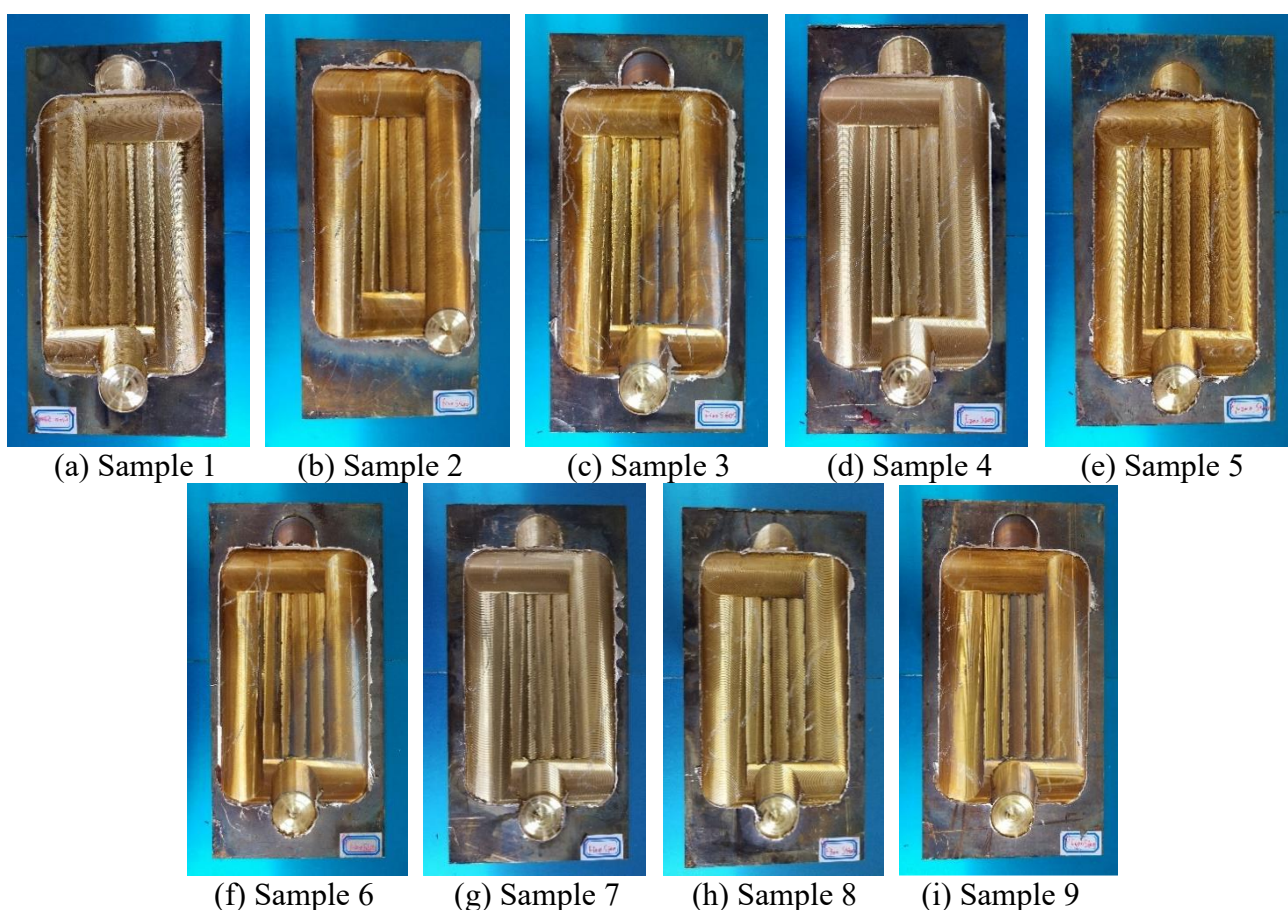


Figure 3. Macro morphologies under different FSSP process parameters: (a) TS=100 mm/min, RS=200 rpm, (b) TS=100 mm/min, RS=400 rpm, (c) TS=100 mm/min, RS=600 rpm, (d) TS=200 mm/min, RS=200 rpm, (e) TS=200 mm/min, RS=400 rpm, (f) TS=200 mm/min, RS=600 rpm, (g) TS=300 mm/min, RS=200 rpm, (h) TS=300 mm/min, RS=400 rpm, and (i) TS=300 mm/min, RS=600 rpm

3.2 Analysis of corrosion resistance

3.2.1 Analysis of electrochemical polarization curve

The polarization curves under different process parameters are depicted in Figure 4.

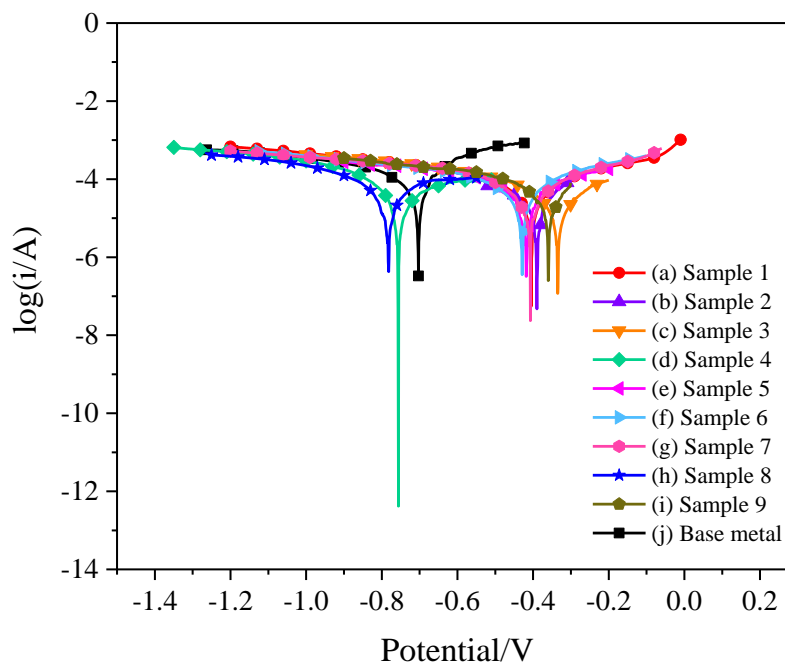


Figure 4. Polarization curves under different FSSP process parameters: (a) TS=100 mm/min, RS=200 rpm, (b) TS=100 mm/min, RS=400 rpm, (c) TS=100 mm/min, RS=600 rpm, (d) TS=200 mm/min, RS=200 rpm, (e) TS=200 mm/min, RS=400 rpm, (f) TS=200 mm/min, RS=600 rpm, (g) TS=300 mm/min, RS=200 rpm, (h) TS=300 mm/min, RS=400 rpm, (i) TS=300 mm/min, RS=600 rpm, and (j) base metal

To avoid man-made operation error, the polarization curves were automatically fitted by CHI660E software matched with the electrochemical workstation. The corrosion potential (E_{corr}) and corrosion current density (I_{corr}) under different FSSP process parameters are listed in Table 3. The more negative the corrosion potential is, the greater the corrosion tendency of the modified surface. The smaller the corrosion current density is, the slower the corrosion rate of the modified surface [25-26]. Therefore, a larger corrosion potential and a smaller corrosion current density are beneficial to obtain a good corrosion resistance of the material [27-28].

Table 3. Corrosion potential and corrosion current density under different FSSP process parameters

Sample Number	1	2	3	4	5	6	7	8	9	Base Metal
E_{corr} (V)	-0.405	-0.39	-0.335	-0.756	-0.418	-0.429	-0.407	-0.782	-0.36	-0.703
I_{corr} (A/cm ²)	9.40e-5	6.67e-5	5.56e-5	6.72e-5	7.12e-5	9.75e-5	9.05e-5	9.61e-5	1.15e-4	1.72e-4

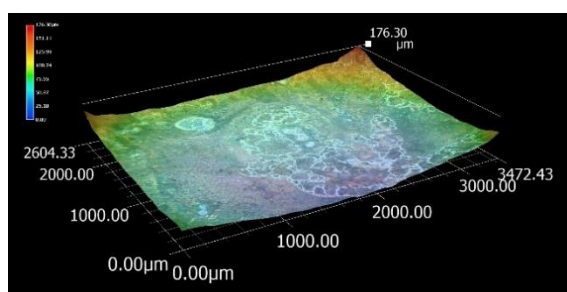
Table 3 shows that sample 3 obtains the largest corrosion potential and the smallest corrosion current density, which indicates that the corrosion resistance of the processed surface is the best when

the traverse speed is 100 mm/min and the rotational speed is 600 rpm. This finding is mainly because the tool advances slowly at a higher rotational speed under such process parameters, resulting in a large amount of heat being generated in the processing area. In this situation, the material is stirred more evenly and is more prone to dynamic recrystallization, which leads to a good corrosion resistance of the processed surface. The refinement of the microstructure produced by friction stir processing is an important reason for the improvement of the corrosion resistance of the material. The refined microstructure helps to form a uniform and dense passivation film on the corrosion surface, thereby improving the corrosion resistance [29-30]. Furthermore, the corrosion current densities of all samples are lower than that of the base metal, which illustrates that the corrosion rate of the H65 copper alloy surface is reduced after FSSP. This proves that FSSP can improve the corrosion resistance of the processed surface to a certain extent, which is consistent with the research conclusion of [31].

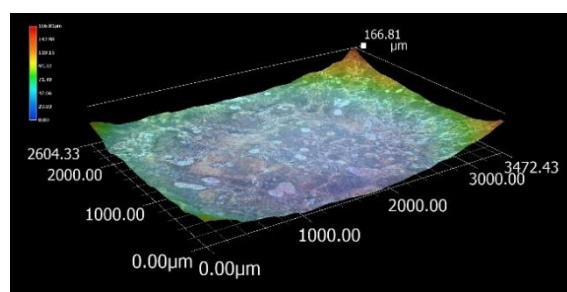
Table 3 also suggests that the corrosion current density decreases with the increase of the rotational speed at a lower traverse speed of 100 mm/min, while there is an opposite trend when the traverse speed is at higher values of 200 mm/min and 300 mm/min. The reason for this phenomenon may be that the heat input of the processing surface plays a leading role at lower traverse speeds. At the same traverse speed, the higher the rotational speed is, the greater the heat input, and the more dynamic recrystallization occurs in the processing area [32]. At higher traverse speeds of 200 mm/min and 300 mm/min, however, the mechanical stirring of the tool plays a leading role due to the decreases in the heat input per unit time of the processed surface. In this case, the higher the rotational speed is, the more obvious the mechanical stirring effect of the tool, the larger the dislocations within the grains, and the faster the corrosion rate of the processed surface.

3.2.2 Analysis of surface corrosion depth

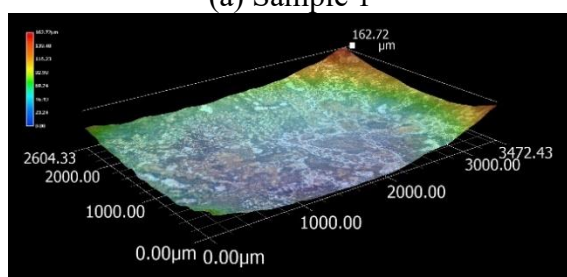
The surface corrosion depths after salt spray corrosion and natural corrosion under different FSSP process parameters are depicted in Figure 5.



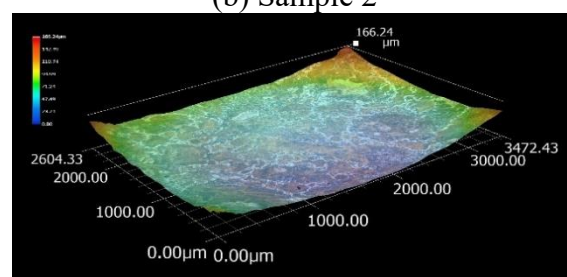
(a) Sample 1



(b) Sample 2



(c) Sample 3



(d) Sample 4

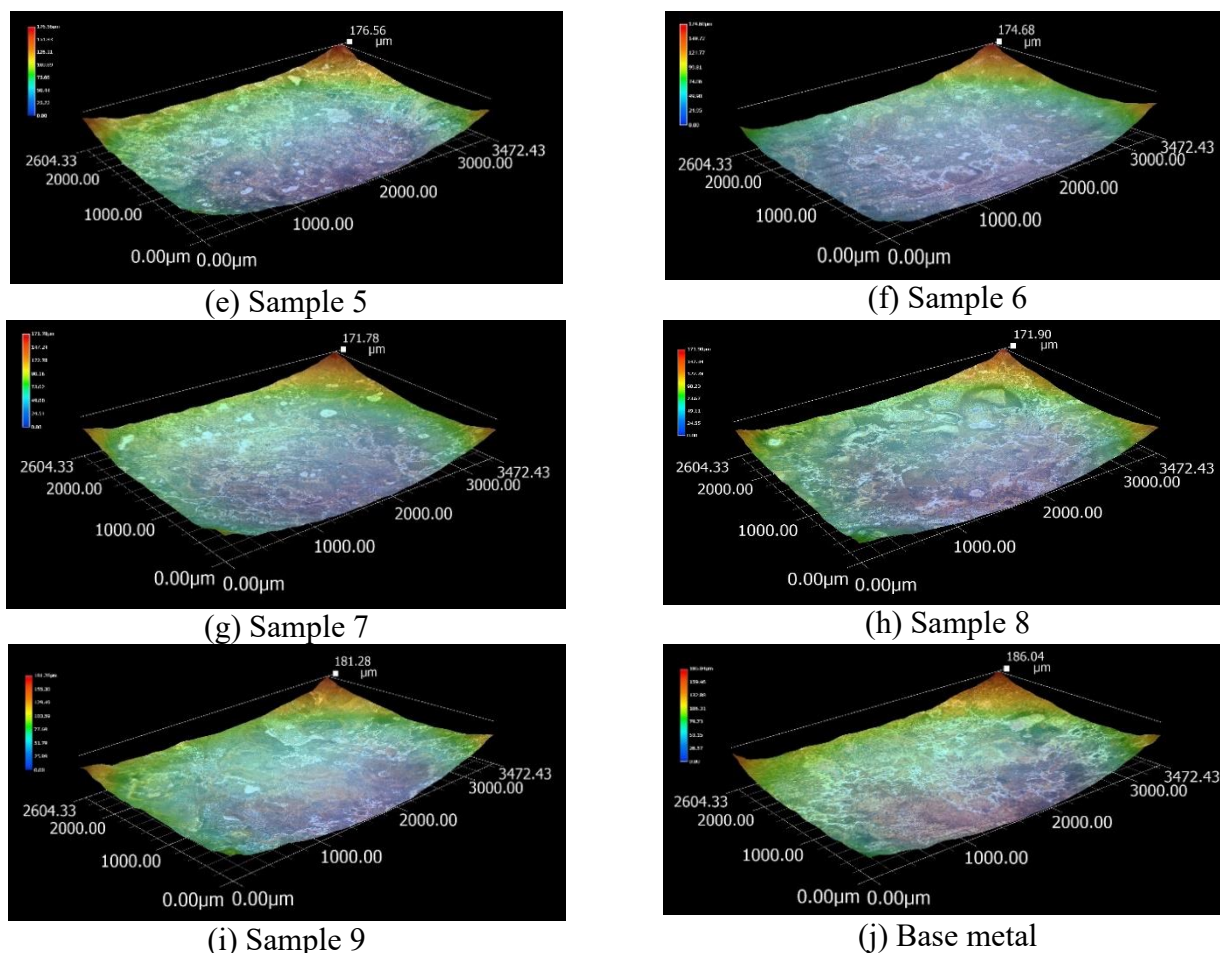


Figure 5. Surface corrosion depths after salt spray corrosion and natural corrosion under different process parameters: (a) TS=100 mm/min, RS=200 rpm, (b) TS=100 mm/min, RS=400 rpm, (c) TS=100 mm/min, RS=600 rpm, (d) TS=200 mm/min, RS=200 rpm, (e) TS=200 mm/min, RS=400 rpm, (f) TS=200 mm/min, RS=600 rpm, (g) TS=300 mm/min, RS=200 rpm, (h) TS=300 mm/min, RS=400 rpm, (i) TS=300 mm/min, RS=600 rpm, and (j) base metal

As shown in Figure 5, sample 3 has the smallest corrosion depth of 162.72 μm , which is 12.53% less than that of the base metal. This value reveals that the corrosion resistance of the modified surface is the best when the traverse speed is 100 mm/min and the rotational speed is 600 rpm, which is consistent with the results of the electrochemical experiment. The corrosion depth of sample 9 is the largest at 181.28 μm , which is lower than that of the base metal. This also proves that the surface corrosion resistance of the H65 copper alloy can be effectively improved by FSSP. On the whole, the corrosion depth of the processed surface is lower when the traverse speed is at a lower value of 100 mm/min than at higher values of 200 mm/min and 300 mm/min, which is mainly due to the material being able to fully agitate at the lower traverse speed [33]. In general, the effect of the process parameters on the surface corrosion resistance of the H65 copper alloy is basically consistent with the electrochemical test results.

3.3 Microstructure analysis of typical process parameters

To reveal the influence mechanism of FSSP process parameters on the surface corrosion

resistance, two samples of typical process parameters (sample 3 with the best corrosion resistance and sample 9 with the worst corrosion resistance) and the base metal were selected to perform EBSD experiments.

Figure 6 shows the grain structures of the base metal, sample 3 and sample 9. Previous studies have confirmed that the grains can be obviously refined by using friction stir processing [34-36]. The reduction in grain size helps to improve the corrosion resistance of the processing area [37-38].

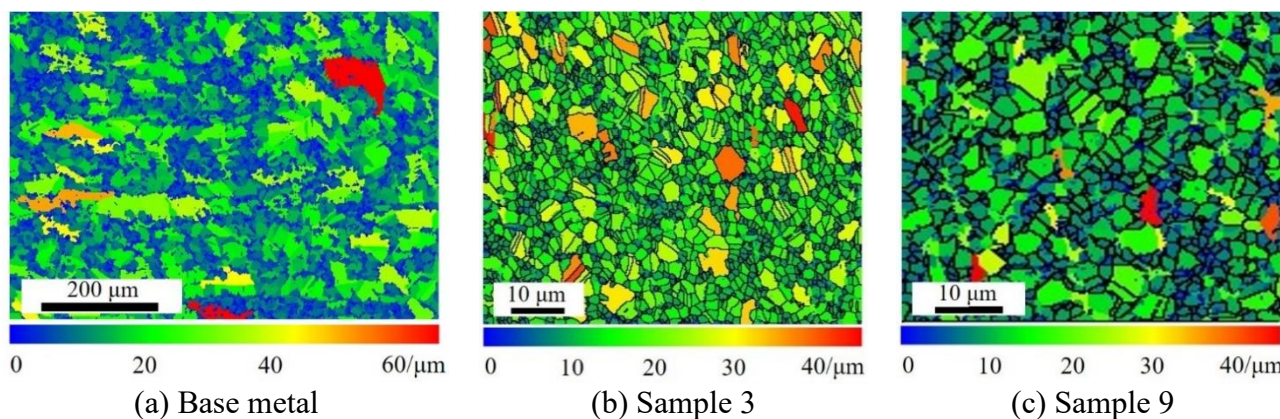


Figure 6. Grain structures of the base metal, sample 3 and sample 9: (a) Base metal, (b) TS=100 mm/min, RS=600 rpm, and (c) TS=300 mm/min, RS=600 rpm

Figure 6 shows that the grains of the base metal are long strips, and the grain size distribution is uneven. Moreover, the grains of sample 3 and sample 9 are significantly refined by comparison with the base metal, and the grain sizes are more uniform. The more refined grains of sample 3 and 9 are mainly due to the severe plastic deformation of the materials in the processing area under the stirring action of the tool, which causes the large-sized grains to be refined [39]. The significant grain refinement is an important reason for the improvement of the corrosion resistance of friction stir processed surfaces.

Figure 7 shows the grain size distributions of sample 3 and sample 9 to further clarify the difference in their grain size.

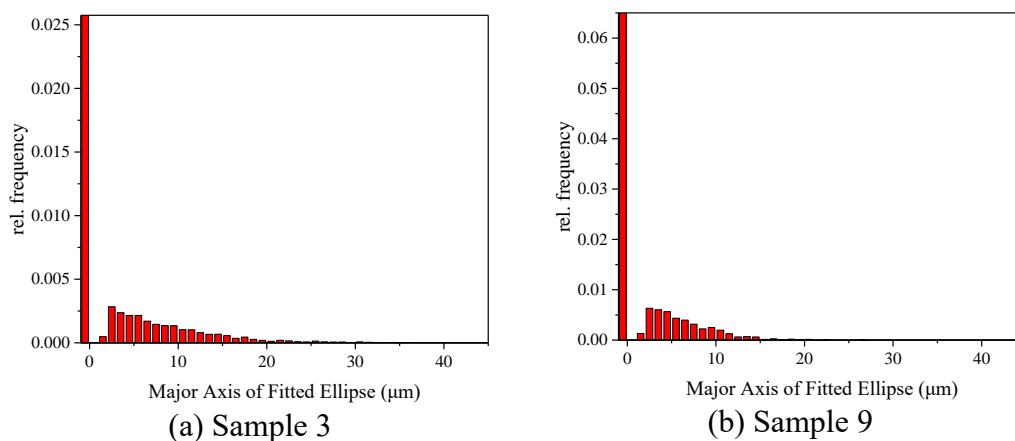


Figure 7. Grain size distributions of sample 3 and sample 9: (a) TS=100 mm/min, RS=600 rpm and (b) TS=300 mm/min, RS=600 rpm

From Figure 7, it can be observed that there are more large grains in sample 3 than in sample 9. This difference is mainly because more heat is generated when the traverse speed is 100 mm/min vs. 300 mm/min, and the grains grow faster at a higher temperature. The effect of temperature on grain growth is consistent with the result of [40].

In the process of FSSP, dynamic recrystallization of varying degrees will occur in the processing area under the combined action of tool mechanical stirring and high temperature [41-43]. This phenomenon has been confirmed in some previous studies [44-45]. The dynamic recrystallization produced during friction stir processing has an important influence on the microstructure evolution and mechanical properties [46]. Zhao et al. studied the effect of dynamic recrystallization on the corrosion sensitivity of brass, and the results indicated that an inadequate recrystallization structure can form corrosion channels, thereby accelerating the corrosion of brass [47]. Therefore, adequate dynamic recrystallization is helpful to improve the corrosion resistance of copper alloys. The dynamic recrystallization maps of the base metal, sample 3 and sample 9 are shown in Figure 8.

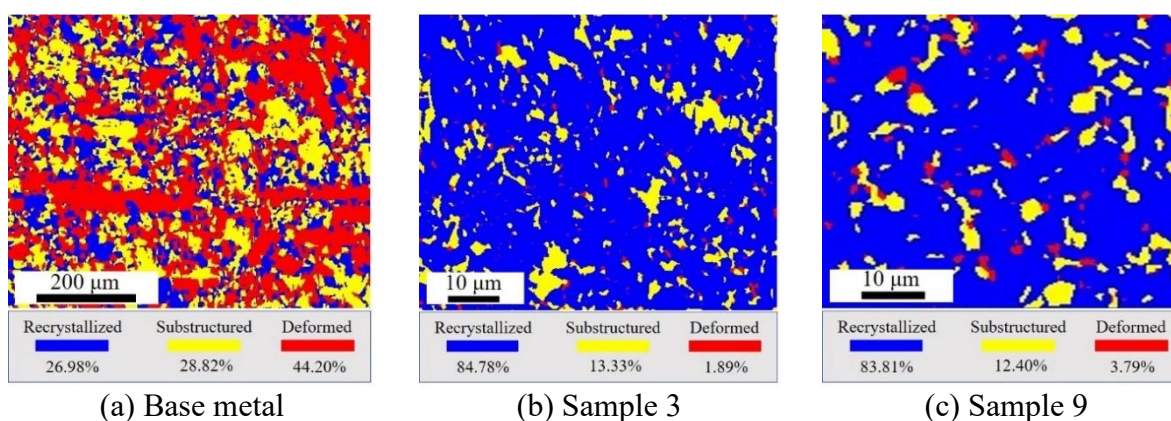


Figure 8. Dynamic recrystallization maps of the base metal, sample 3 and sample 9: (a) Base metal, (b) TS=100 mm/min, RS=600 rpm, and (c) TS=300 mm/min, RS=600 rpm

Figure 8 shows that the recrystallized percentage of the base metal is only 26.98%, and there are a large number of subcrystals. The recrystallization percentages of sample 3 and sample 9 are significantly higher than that of the base metal. Sample 3 obtains a larger recrystallized percentage (84.78%) and a smaller deformed percentage (1.89%) than sample 9, which indicates that dynamic recrystallization occurs adequately under the process parameters of sample 3. This is mainly because more heat is generated when the traverse speed is 100 mm/min and the rotational speed is 600 rpm. At the same time, it is also related to the severe plastic deformation caused by the stirring of the tool [48].

Figure 9 and Figure 10 show the dislocation density maps and the dislocation density distributions of the base metal, sample 3 and sample 9.

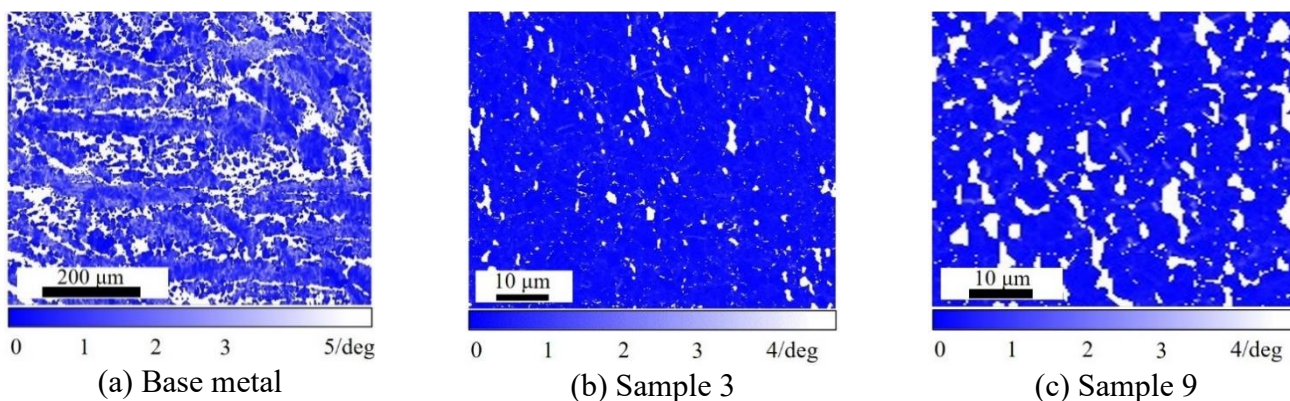


Figure 9. Dislocation density maps of the base metal, sample 3 and sample 9: (a) Base metal, (b) TS=100 mm/min, RS=600 rpm, and (c) TS=300 mm/min, RS=600 rpm

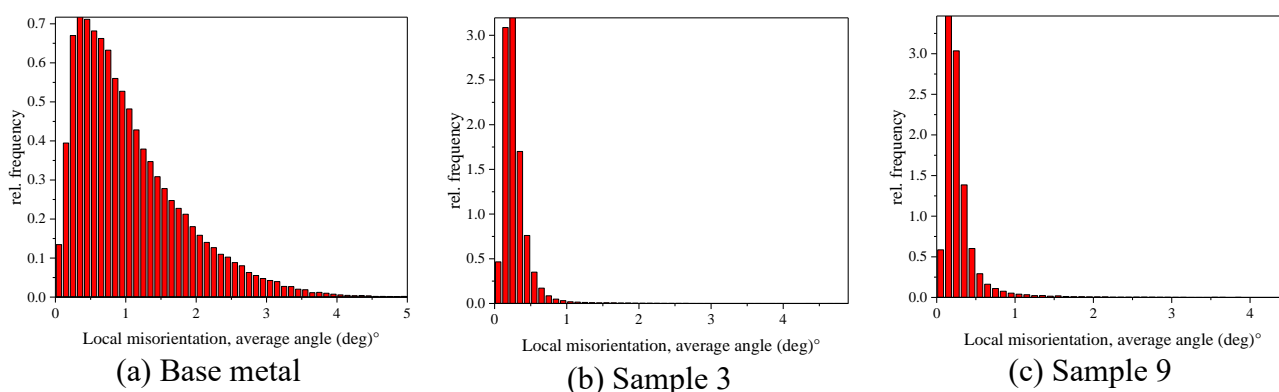


Figure 10. Dislocation density distributions of the base metal, sample 3 and sample 9: (a) Base metal, (b) TS=100 mm/min, RS=600 rpm, and (c) TS=300 mm/min, RS=600 rpm

Dislocation is an internal microdefect of crystalline material that has an important impact on the corrosion resistance of the material [49]. The higher the dislocation density, the more serious the microdefects, and the easier the material will be corroded [50]. Studies [51-54] have also confirmed this point; that is, the greater the dislocation density is, the faster the dissolution rate of the metal, and the larger the corrosion rate of the material. Therefore, a smaller dislocation density is desirable to obtain good corrosion resistance. From Figure 9 and Figure 10, it can be observed that the dislocation density of the base metal is the largest, which is one of the important reasons why the corrosion resistance of the base metal is poor. The dislocation densities of sample 3 and sample 9 are significantly reduced compared with that of the base metal. This also demonstrates that FSSP has a better effect on improving the microstructure and properties of copper alloy, which is consistent with the research result of [55]. Furthermore, the dislocation density of sample 9 is slightly higher than that of sample 3. This is because the traverse speed of sample 9 is faster, resulting in the heat input being relatively reduced in the processing area. Under this condition, the strong mechanical stirring effect of the tool enhances the dislocation within the grains, which accelerates the metal dissolution rate of the corrosion surface, resulting in the corrosion resistance of sample 9 being lower than that of sample 3.

In summary, when the traverse speed is 100 mm/min and the rotational speed is 600 rpm, the grains are obviously refined compared to the base metal, the material undergoes adequate dynamic recrystallization under the action of high heat input, and the dislocation density within the grains is significantly reduced, which effectively improves the corrosion resistance of the processed surface.

4. CONCLUSIONS

In this study, the corrosion resistance of the H65 copper alloy surface was investigated under different FSSP process parameters. The microstructures from typical process parameters and the base metal were analyzed by EBSD experiments. The main conclusions are as follows:

(1) The corrosion resistance of the H65 copper alloy surface is improved to various degrees under different FSSP process parameters, which indicates that FSSP is an effective and simple surface modification method.

(2) When the traverse speed is 100 mm/min and the rotational speed is 600 rpm, the corrosion resistance of the H65 copper alloy surface is the best. Under this condition, the corrosion current density is reduced by 67.67% and the corrosion depth is reduced by 12.53% compared with the base metal.

(3) When the traverse speed is 100 mm/min and the rotational speed is 600 rpm, the recrystallization percentage reaches 84.78%, which is much higher than 26.98% for the base metal. The grain size and dislocation density are also significantly lower than those of the base metal.

ACKNOWLEDGMENTS

The authors gratefully acknowledge the support from the Open Research Project of Anhui Simulation Design and Modern Manufacture Engineering Technology Research Center (No. SGCZXZD1803, SGCZXZD2001), the Natural Science Foundation of Anhui Higher Education Institutions (No. KJHS2019B15, KJ2020A0687), the Anhui Provincial Excellent Young Talents Support General Project (No. GXYQ2019086) and the Key Research and Development Project from Anhui Province of China (No. 202004A05020025, 202104B11020011).

References

1. Y. F. Geng, Y. J. Ban, B. J. Wang, X. Li, K. X. Song, Y. Zhang, Y. L. Jia, B. H. Tian, Y. Liu, A. A. Volinsky, *Journal of Materials Research and Technology*, 9 (2020) 11918.
2. A. K. Shukla, S. V. S. Narayana Murty, S. C. Sharma, K. Mondal, *Materials and Design*, 75 (2015) 57.
3. Y. Zhang, H. L. Sun, A. A. Volinsky, B. H. Tian, K. X. Song, B. J. Wang, Y. Liu, *Vacuum*, 146 (2017) 35.
4. X. L. Guo, Z. Xiao, W. T. Qiu, Z. Li, Z. Q. Zhao, X. Wang, Y. B. Jiang, *Materials Science and Engineering A*, 749 (2019) 281.
5. B. M. Luo, D. X. Li, C. Zhao, Z. Wang, Z. Q. Luo, W. W. Zhang, *Materials Science and Engineering A*, 746 (2019) 154.
6. S. Xu, H. D. Fu, Y. T. Wang, J. X. Xie, *Materials Science and Engineering A*, 726 (2018) 208.
7. X. L. Sun, J. C. Jie, P. F. Wang, B. L. Qin, X. D. Ma, T. M. Wang, T. J. Li, *Materials Science and Engineering A*, 740 (2019) 165.
8. Z. Q. Wang, Y. B. Zhong, G. H. Cao, C. Wang, J. Wang, W. L. Ren, Z. S. Lei, Z. M. Ren, *Journal*

- of Alloys and Compounds*, 479 (2009) 303.
9. K. M. Liu, Z. Y. Jiang, J. W. Zhao, J. Zou, L. Lu, D. P. Lu, *Metallurgical and Materials Transactions A*, 46 (2015) 2255.
 10. T. Hu, J.H. Chen, J.Z. Liu, Z.R. Liu, C.L. Wu, *Acta Materialia*, 61 (2013) 1210.
 11. B. P. Singh, B. K. Jena, S. Bhattacharjee, L. Besra, *Surface and Coatings Technology*, 232 (2013) 475.
 12. V. I. Chukwuike, O. G. Echem, S. Prabhakaran, S. AnandKumar, R. C. Barik, *Corrosion Science*, 179 (2021) 109156.
 13. G. X. Hu, Z. X. Xu, J. J. Liu, Y. H. Li, *Surface and Coatings Technology*, 203 (2009) 3392.
 14. X. Q. Xu, L. Q. Zhu, W. P. Li, H. C. Liu, *Applied Surface Science*, 257 (2011) 5524.
 15. A. R. Eivani, M. Mehdizade, S. Chabok, J. Zhou, *Journal of Materials Research and Technology*, 12 (2021) 1946.
 16. Q. H. Zang, H. M. Chen, J. Zhang, L. Wang, S. J. Chen, Y. X. Jin, *Journal of Materials Research and Technology*, 14 (2021) 195.
 17. C. Y. Ma, L. Zhou, R. X. Zhang, D. G. Li, F. Y. Shu, X. G. Song, Y. Q. Zhao, *Journal of Materials Research and Technology*, 9 (2020) 8296.
 18. L. Pan, C. T. Kwok, K. H. Lo, *Surface and Coatings Technology*, 357 (2019) 339.
 19. F. J. Liu, Y. Ji, Z. Y. Sun, J. B. Liu, Y. X. Bai, Z. K. Shen, *Journal of Alloys and Compounds*, 829 (2020) 154452.
 20. J. J. Pang, F. C. Liu, J. Liu, M. J. Tan, D. J. Blackwood, *Corrosion Science*, 106 (2016) 217.
 21. K. Yang, W. Y. Li, Y. X. Xu, X. W. Yang, *Journal of Alloys and Compounds*, 774 (2019) 1223.
 22. J. Paulo Davim. *Welding Technology*, Springer, (2021) Cham, Germany.
 23. W. W. Song, D. W. Zuo, X. J. Xu, H. F. Wang, S. R. Liu, *International Journal of Electrochemical Science*, 14 (2019) 7026.
 24. W. W. Song, Study on modification technology and mechanism of H62 copper alloy layer by friction stir surface processing technology and implanting particles, *Jiangsu University*, (2017) Zhenjiang, China.
 25. C. N. Cao, Principles of electrochemistry of corrosion, *Chemical Industry Press*, (2008) Beijing, China.
 26. J. J. Shi, Research on the preparation process of high corrosion resistance 7 series aluminum alloy, *Hefei University of Technology*, (2018) Hefei, China.
 27. M. Wang, Q. Liu, Y. X. Zhang, N. N. Zhang, M. P. Liu, *Chinese Journal of Materials Research*, 29 (2015) 589.
 28. C. B. Shen, Y. Peng, Y. Chen, N. Y. Jiang, *Transactions of the China Welding Institution*, 38 (2017) 59.
 29. C. C. Zhang, H. Wu, X. Y. Yu, *Surface Technology*, 50 (2021) 315.
 30. L. Tong, Q. L. Xu, Y. P. Ma, C. L. Liu, *Journal of Chongqing University of Technology*, 30 (2016) 52.
 31. W. W. Song, X. J. Xu, D. W. Zuo, J. L. Wang, *Anti-Corrosion Methods and Materials*, 63 (2016) 190.
 32. C. Y. Jin, Z. S. Cui, *Journal of Yangzhou University*, 14 (2011) 60.
 33. F. F. Chen, H. J. Huang, P. Xue, Z. Y. Ma, *Chinese Journal of Materials Research*, 32 (2018) 1.
 34. Y. F. Hou, C. Y. Liu, B. Zhang, L. L. Wei, H. T. Dai, Z. Y. Ma, *Materials Science and Engineering: A*, 785 (2020) 139393.
 35. A. Heidarpour, Y. Mazaheri, M. Roknian, S. Ghasemi, *Journal of Alloys and Compounds*, 783 (2019) 886.
 36. A. Heidarzadeh, H. Pouraliakbar, S. Mahdavi, M. R. Jandaghi, *Ceramics International*, 44 (2018) 3128.
 37. H. Seifiyan, M.H. Sohi, M. Ansari, D. Ahmadkhaniha, M. Saremi, *Journal of Magnesium and Alloys*, 7 (2019) 605.

38. J. S. Liao, M. Hotta, N. Yamamoto, *Corrosion Science*, 61 (2012) 208.
39. H. Mazaheri, H. J. Aval, R. Jamaati, *Materials Science and Engineering: A*, 826 (2021) 141958.
40. S. F. Liu, Z. F. Zhou, C. F. Li, *Journal of Aeronautical Materials*, 35 (2015) 39.
41. Y. Li, P. J. Hou, Z. G. Wu, Z. L. Feng, Y. Ren, H. Choo, *Materials & Design*, 202 (2021) 109562.
42. S. Biswas, B. Beausir, L. S. Toth, S. Suwas, *Acta Materialia*, 61 (2013) 5263.
43. R. L. Xin, B. Li, A. L. Liao, Z. Zhou, Q. Liu, *Metallurgical and Materials Transactions A-Physical Metallurgy and Materials Science*, 43 (2012) 2500.
44. Z. H. Zhang, W. Y. Li, Y. Feng, J. L. Li, Y. J. Chao, *Acta Materialia*, 92 (2015) 117.
45. Y. S. Sato, H. Kokawa, M. Enomoto, *Metallurgical and Materials Transactions A*, 30 (1999) 2429.
46. Y. X. Huang, Y. B. Wang, X. C. Meng, L. Wan, J. Cao, L. Zhou, J. C. Feng, *Journal of Materials Processing Technology*, 249 (2017) 331.
47. Y. H. Zhao, L. Y. Lin, Z. H. Wang, *Journal of Chinese Society for Corrosion and Protection*, 32 (2012) 102.
48. T. R. McNelley, S. Swaminathan, J. Q. Su, *Scripta Materialia*, 58 (2008) 349.
49. S. S. Mirian Mehrian, M. Rahsepar, F. Khodabakhshi, A.P. Gerlich, *Surface and Coatings Technology*, 405 (2021) 126647.
50. W. Y. Lai, X. Xu, Z. Q. Bai, C. X. Yin, X. Q. Xu, Y. Han, *Materials for Mechanical Engineering*, 40 (2016) 84.
51. D. J. Li, D. S. Guo, Y. F. Ju, W. Y. Liang, X. T. Zhang, F. Z. Ren, *Transactions of Materials and Heat Treatment*, 42 (2021) 115.
52. D. J. Sprouster, W. S. Cunningham, G. P. Halada, H. F. Yan, A. Pattammattel, X. J. Huang, D. Olds, M. Tilton, Y. S. Chu, E. Dooryhee, G. P. Manogharan, J. R. Trelewicz, *Additive Manufacturing*, 47 (2021) 102263.
53. M. Rahsepar, H. Jarahimoghadam, *Materials Science and Engineering: A*, 671 (2016) 214.
54. V. Pandey, J. K. Singh, K. Chattopadhyay, N. C. Santhi Srinivas, V. Singh, *Journal of Alloys and Compounds*, 723 (2017) 826.
55. W. W. Song, X. J. Xu, S. R. Liu, J. F. Pu, X. L. Ge, *Materials Transactions*, 60 (2019) 765.

© 2022 The Authors. Published by ESG (www.electrochemsci.org). This article is an open access article distributed under the terms and conditions of the Creative Commons Attribution license (<http://creativecommons.org/licenses/by/4.0/>).